Numerical Model of Calcium Valence Electrons

Jun Wang

Dec. 20, 2018

1 Overview

This project is building a quantum mechanical model of the two valence electrons in a Calcium atom. The purpose is to obtain full knowledge of states $[\mathrm{Ar}]nln'l'\ ^{2S+1}L_J$, including

- Stark shift of a high Rydberg state
- Linewidth of a high Rydberg state
- Energy difference between states of interest

The Hilbert space of the two-particle system $\mathcal{H}$ is the antisymmetrized direct product of two single-body Hilbert space $\mathcal{A}(\mathcal{H}_1 \otimes \mathcal{H}_1)$. The total Hamiltonian is

$$H = \sum_{k=1,2} h_0(k) + V + H_{\mathrm{SOC}}, \tag{1}$$

$$V = \frac{e^2}{4\pi\epsilon_0|\boldsymbol{r}_1 - \boldsymbol{r}_2|}, \tag{2}$$

$$h_0 = \frac{-\hbar^2}{2\mu}\boldsymbol{\nabla}^2 + U(r) = \frac{-\hbar^2}{2\mu r^2}\partial_r r^2 \partial_r + \frac{\boldsymbol{l}^2}{2\mu r^2} + U(r), \tag{3}$$

$$H_{\mathrm{SOC}} = \sum_{k=1,2} \xi(r_k)\boldsymbol{s}_k \cdot \boldsymbol{l}_k + \sum_{k_1 \neq k_2} \eta(r_{k_1}, r_{k_2}, |\boldsymbol{r}_1 - \boldsymbol{r}_2|)\boldsymbol{s}_{k_1} \cdot \boldsymbol{l}_{k_2}\ , \tag{4}$$

where $U(r)$ is the model potential produced by the Ca^{2+} core for a single electron, depending only on the radial distance. $\xi(r) = \frac{1}{2m_e^2c^2}\frac{\mathrm{d}U}{r\mathrm{d}r}$, and as for the inter-electron spin-orbit coupling coefficient $\eta(r_1, r_2, |\boldsymbol{r}_1 - \boldsymbol{r}_2|)$, I do not have its specific form but supposedly it depends on their distance to the center and their relative distance.

1.1 Units and Notation Conventions

The numerical implementation is in (Hatree) Atomic Units, which is elaborated in Tab. 1 . In this

Table 1: Useful expressions and values in (Hatree) Atomic Units, extracted from Ref. [1] .

Dimension	Expression(s)	Value in SI	Value in other units
Length	$a_0 = \frac{4\pi\epsilon_0\hbar^2}{m_e e^2}$	0.5292Å	
Angular momentum	$\hbar$	1.055×10^{-34}J·s	
Mass	m_e	9.109×10^{-31}kg	
Energy	$E_H = \frac{m_e e^4}{(4\pi\epsilon_0\hbar)^2} = \frac{\hbar^2}{m_e a_0^2} = \alpha^2 m_e c^2$	4.360×10^{-18}J	27.21eV
Frequecy	$E_H/\hbar$	4.134×10^{16}Hz	
Velocity	$E_H a_0/\hbar = \frac{e^2}{4\pi\epsilon_0\hbar} = \alpha c$	2.188×10^{6}m/s	7.297×10^{-3}c

unit system, the terms in the Hamiltonian are

$$V = \frac{1}{|\boldsymbol{r}_1 - \boldsymbol{r}_2|}, \tag{5}$$

$$h_0 = \frac{-1}{2\mu r^2}\partial_r r^2 \partial_r + \frac{\boldsymbol{l}^2}{2\mu r^2} + U(r), \tag{6}$$

$$\xi(r) = \frac{\alpha^2}{2}\frac{\mathrm{d}U}{r\mathrm{d}r}, \tag{7}$$

where $\alpha = \frac{e^2}{4\pi\epsilon_0\hbar c}$ is the fine-structure constant. $U(+\infty) = 0$ indicates that the reference point of the total energy corresponds to the state where both the valence electrons are ionized, i.e. Ca III (^{1}S$_0$) [2].

Aside from the (Hatree) Atomic Unit, there are some other conventions about notation:

- ϕ is an orbital wavefunction, while ψ is a total wavefunction taking 2 by 1 column vector values;
- Some quantities are capitalized to stress that they are of two-particle system, distinguished from their single-particle counterparts, e.g. $E, \boldsymbol{L}, \Phi, \Psi$ from $\epsilon, \boldsymbol{l}, \phi, \psi$.
- $\mathcal{P}_{12}$ refers to the transposition of the identities of the two electrons. Note that for a total wavefunction Ψ it transposes the tensor indices besides swaping $\boldsymbol{r}_1, \boldsymbol{r}_2$;
- $\mathcal{A}$ is the normed antisymmetrization operator. For any (orbital or total) two-body wavefunction Ψ

$$(\mathcal{A}\Psi) \equiv (\Psi - \mathcal{P}_{12}\Psi)/||\Psi - \mathcal{P}_{12}\Psi||_2 \tag{8}$$

$$||\Psi||_2 \equiv \sqrt{\int \mathrm{d}^3\boldsymbol{r}_1 \mathrm{d}^3\boldsymbol{r}_2 \Psi(\boldsymbol{r}_1, \boldsymbol{r}_2)^\dagger \Psi(\boldsymbol{r}_1, \boldsymbol{r}_2)} \tag{9}$$

1.2 Implementation

It is straightforward to verify that $0 = [V, \boldsymbol{L}] = [V, \boldsymbol{S}] = [V, \boldsymbol{J}]$, and $\forall k_1, k_2 \in \{1, 2\}, \boldsymbol{s}_{k_1} \cdot \boldsymbol{l}_{k_2}$ commutes with $\boldsymbol{L}^2, \boldsymbol{S}^2$ and $\boldsymbol{J}$. Therefore $H, \boldsymbol{L}^2, \boldsymbol{S}^2, \boldsymbol{J}^2, J_z$ comprise a commutable set of conservatives. Even the orbit-orbit coupling $\boldsymbol{l}_1 \cdot \boldsymbol{l}_2$ and spin-spin coupling $\boldsymbol{s}_1 \cdot \boldsymbol{s}_2$ terms, which are neglected at the very beginning, commute with $\boldsymbol{L}^2, \boldsymbol{S}^2, \boldsymbol{J}^2, J_z$. As a result, an atom (and atomic ion) state can be

marked by quantum numbers L, S, J, M_J, and M_J is usually left out when describing a level due to degeneracy.

In lighter elements, the deviation of an energy level from the product state energy is dominated by electrostatic interactions V, so LS coupling is adopted. However $\boldsymbol{L}^2, \boldsymbol{S}^2, \boldsymbol{J}^2, J_z$ is not a complete set, so the eigenstate is a superposition of different electron configurations in the eigen subspace marked by L, S, J, M_J, and the state marked by $(n_1, l_1, n_2, l_2), L, S, J, M_J$ is not an eigenstate of $\boldsymbol{l}_1^2, \boldsymbol{l}_2^2$ but the eigenstate that overlaps the most with the electron configuration (n_1, l_1, n_2, l_2). The workflow for obtaining it is

1. Solve all single electron states from $h_0\psi = \epsilon\psi$;
2. In an eigen subspace marked by L, S, J, M_J:
   (1) Compute the matrix elements of V and H_{SOC};
   (2) Choose a set of electron configurations that are relevant to the perturbation of the state of interest, as the computational basis;
   (3) Construct the matrix of H and diagonalize;
   (4) Pick the eigenvector that overlaps the most with the electron configuration of interest.

The codes and references are available on Github.

2 Single Particle States

2.1 Model Potential $U(r)$

The Klapisch form is adopted for the model potential $U(r)$, including a screening term and a polarization term

$$U(r) \equiv \frac{-1}{r}(2 + 18\mathrm{e}^{-a_1^{(l)}r} - r(a_3^{(l)} + a_4^{(l)}r)\mathrm{e}^{-a_2^{(l)}r}) - \frac{\alpha_d}{2r^4}(1 - \mathrm{e}^{-(r/r_c^{(l)})^6}), \tag{10}$$

and the parameters a_1, a_2, a_3, a_4, r_c are l-dependent. The dipole polarizability of the Ca^{2+} core α_d is not. Table 2 lists an optimized set that is restricted to $\alpha_d = 3.5, a_4 = 0$, A comprehensive list

Table 2: 4-parameter model potential of Klapisch form optimized by [3]

l	a_1	a_2	a_3	r_c
0	4.0099	2.1315	-13.023	1.6352
1	4.2056	2.0186	-12.658	1.5177
2	3.5058	2.2648	-12.399	1.6187
≥ 3	3.7741	3.1848	-13.232	0.7150

of α_d values could be found in [4], including an experimental value [5] $\alpha_d = 3.26$ and theoretical values centered around this one. Since [3] cited nothing for its $\alpha_d = 3.5$, optimization for $\alpha_d = 3.26$ is potentially necessary. For now, just keep it in mind.

2.2 Radial Equation

Since h_0 has nothing to do with spin and $0 = [h_0, \boldsymbol{l}^2] = [h_0, l_z]$, separating variables in $h_0\psi = \epsilon\psi$, one sets

$$\psi_{n,l,m,m_s}(\boldsymbol{r}) = \phi_{n,l,m}(\boldsymbol{r})\chi(m_s) = \frac{u_{nl}(r)}{r} Y_{lm}(\boldsymbol{r}/r)\chi(m_s), \tag{11}$$

where u_{nl} is the radial function to be solved, and

$$Y_{lm}(\theta,\varphi) = \sqrt{\frac{(2l+1)(l-m)!}{4\pi(l+m)!}} \mathrm{e}^{\mathrm{i}m\varphi} P_l^m(\cos\theta); \tag{12}$$

$$\chi(m_s) = (\delta_{m_s,1/2}, \delta_{m_s,-1/2})^T. \tag{13}$$

From the single particle Schrödinger equation, one obtains the radial equation:

$$\epsilon_{n,l}\frac{u_{nl}(r)}{r} = \left(\frac{-1}{2\mu r^2}\partial_r r^2 \partial_r + \frac{l(l+1)}{2\mu r^2} + U(r)\right)\frac{u_{nl}(r)}{r}, \tag{14}$$

$$\text{i.e. } \epsilon_{n,l}u_{nl}(r) = \left(\frac{-1}{2\mu}\frac{\mathrm{d}^2}{\mathrm{d}r^2} + \frac{l(l+1)}{2\mu r^2} + U(r)\right)u_{nl}(r), \tag{15}$$

$$\text{i.e. } \frac{\mathrm{d}^2 u_{nl}(r)}{\mathrm{d}r^2} + \gamma(r)u_{nl}(r) = 0, \quad \gamma(r) = 2\mu(\epsilon_{n,l} - U(r)) - \frac{l(l+1)}{r^2}, \tag{16}$$

which also indicates that $u_{nl}(r) \in \mathbb{R}$.

In order for better convergence properties, transform eq.(16) into the differential equation of variable $y(x) = x^{-1/2}u(x^2), x = \sqrt{r}$,

$$\frac{\mathrm{d}^2 y}{\mathrm{d}x^2} + g(x)y(x) = 0, \quad g(x) = 4x^2\gamma(x^2) - \frac{3}{4x^2} \tag{17}$$

Discretizing with Numerov difference form and gridding x with even step length h

$$\frac{y_{k-1} - 2y_k + y_{k+1}}{h^2} + \frac{1}{12}g_{k-1}y_{k-1} + \frac{10}{12}g_k y_k + \frac{1}{12}g_{k+1}y_{k+1} = 0 \tag{18}$$

$$\text{i.e. } (1 + \frac{h^2}{12}g_{k-1})y_{k-1} + (-2 + \frac{10h^2}{12}g_k)y_k + (1 + \frac{h^2}{12}g_{k+1})y_{k+1} = 0 \tag{19}$$

Recall the definitions of $g(x), \gamma(r)$ in Eq.(17)(16), and define $W(x)$, one obtains

$$g(x) = 8\mu x^2\epsilon_{n,l} - W(x), \quad W(x) = 8\mu U(x^2) + \frac{4(l+1/4)(l+3/4)}{x^2} \tag{20}$$

I wrote a python module `numerov` in C++ to either integrate the radial function or solve the eigenequation of the radial function. For Mac OS X, the .so file is ready in `./Numerov`; For other Unix systems, one can simply run `./pyCppbuild` in the directory of `./Numerov` to obtain the corresponding .so file. To use this module, one can either copy this .so file to the current working path or claim `sys.path.append("[path of the Dev folder]/Numerov")` in the python scripts.

The module also supports solving the radial function in the Schrödinger equation with SOC term:

$$h\left\{\frac{u_{nlj}(r)}{r}\sum_m \langle l, m_l, \frac{1}{2}, m - m_l | j, m\rangle Y_{lm_l}(\frac{\boldsymbol{r}}{r})\chi(m - m_l)\rangle\right\} = \epsilon_{n,l,j}\sum_{m_l}\langle l, m_l, \frac{1}{2}, m - m_l | j, m\rangle Y_{lm_l}(\frac{\boldsymbol{r}}{r})\chi(m - m_l)$$

Please refer to the documentation of the functions `numerov.integrate` and `numerov.eigensolve`.

2.2.1 Integration

The integration function `numerov.integrate` simply integrates inwards according to eq.(19). Because the error of the model potential is smaller outside the Ca^{2+} region, integrating inwards is more credible than outwards.

$$y_{k-1} = \left(1 + \frac{h^2}{12} g_{k-1}\right)^{-1} \left((2 - \frac{10h^2}{12} g_k) y_k - (1 + \frac{h^2}{12} g_{k+1}) y_{k+1}\right) \tag{21}$$

2.2.2 Solving eigen equation

In Eq.(19), moving all the ϵ terms to the r.h.s

$$(1 - \frac{h^2}{12} W_{k-1}) y_{k-1} + (-2 - \frac{10h^2}{12} W_k) y_k + (1 - \frac{h^2}{12} W_{k+1}) y_{k+1} = -\frac{2\mu}{3} \epsilon (r_{k-1} y_{k-1} + r_k y_k + r_{k+1} y_{k+1}), \tag{22}$$

it is now in the form $A \cdot x = \lambda M \cdot x$, where both A, M are tri-diagonal real matrices and thus can be easily LU decomposed. Avoiding ill-conditioned M, both sides of Eq.(22) are divided by r_k before applying the subroutine that solves λ, x from $A \cdot x = \lambda M \cdot x$. For details about this subroutine, please refer to App. A.

2.3 Assessment of model parameters, in terms of CaII spectra

In order to assess the model parameters qualitatively, one should look into the mismatch between the solved eigenenergies and the experimental values. What we need in the following computation is the eigenbasis of h_0, while the experimental values in Ref. [2] are with fine structure. From the fine structure split

$$\langle \boldsymbol{l} \cdot \boldsymbol{s} \rangle = \begin{cases} \frac{l}{2} & \text{if } j = l + \frac{1}{2} \\ \frac{-(l+1)}{2} & \text{if } j = l - \frac{1}{2}, \end{cases} \tag{23}$$

one obtains

$$\epsilon_{n,l} = \begin{cases} \epsilon_{n,0,1/2} & \text{if } l = 0, \\ \frac{l+1}{2l+1} \epsilon_{n,l,l+1/2} + \frac{l}{2l+1} \epsilon_{n,l,l-1/2} & \text{if } l > 0, \end{cases} \tag{24}$$

`./specs/CaII_ebar.npz` includes these averaged $\epsilon_{n,l}$ processed from $\epsilon_{n,l,j}$ data in `./specs/CaII.npz`. With the model parameters in Tab. 2, the relative errors of eigenenergies, with respect to the experimental $\epsilon_{n,l}$ data, square root meaned over different n for the same l, are no larger than 5×10^{-4}.

2.4 Extrapolation with quantum defects

Either integrate or solve the eigen equation for radial function u_{nl} or single-particle wavefunction ψ_{n,l,m,m_s}, at least an approximate value of energy $\epsilon_{n,l}$ is necessary. The experimental values [2], however, are limited after all. In order for ψ_{n,l,m,m_s} of arbitrary n, l, I extrapolated the experimental $\epsilon_{n,l}$ with an l-dependent quantum defect:

$$\epsilon_{n,l} = \frac{-1}{2(n - \delta_l)^2}. \tag{25}$$

The linear dependence of $2/\sqrt{-2\epsilon_{n,l}}$ on n is quite obvious in Fig.1 , namely, $\epsilon_{n,l} = \frac{-1}{2(\alpha_l n - \delta_l)^2}$ with

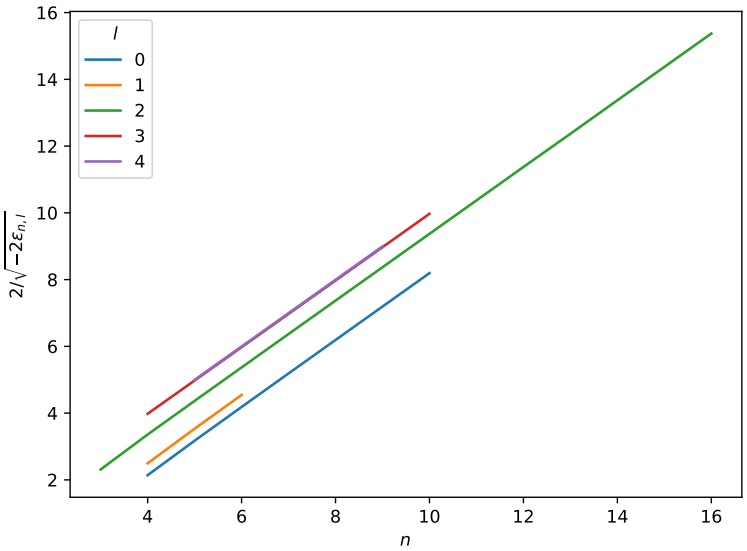

Figure 1: Fitting quantum defect parameters from experimental values of CaII energies.

α_l, δ_l being the fitting parameters. The fitting results are stored in `./specs/ebar_quant_defect.pickle` , and unsurprisingly all α_l are all close to unity. Note that $l = 3, 4$ are close enough to each other, I assume $l > 4$ has the same quantum defect as $l = 4$.

Now for arbitrary n, l, one has the energy $\epsilon_{n,l}$, which is the experimental value if could be found or extrapolated otherwise. This is implemented in `request_energy` in `./LS.py`, and the radial wavefunction u_{nl} is subsequently obtained via Numerov integration, implemented in `request_ur` .

3 Coupling to Two-Particle States

Now the single particle basis $\{\psi_{n,l,m,m_s} | n \geq 3; l < n,\ l \geq 0 \text{ if } n > 3 \text{ else } 2; |m| \leq l; m_s = \pm\frac{1}{2}\}$ is ready. The Hilbert space $\mathcal{H}$ can be spanned by the antisymmetrized direct products $\mathcal{A}(\psi_{n1,l1,m1,m_s1} \otimes \psi_{n2,l2,m2,m_s2})$, or any complete set of linear combination of them. By LS coupling it means the basis $\mathcal{B}$ is structured as

$$\mathcal{B} \equiv \{\mathcal{B}_{L,S,J,M_J} | L \in \mathbb{N}; S = 0, 1; J = |L - S|, \cdots, L + S; M_J = -J, \cdots, +J\} , \tag{26}$$

$$\mathcal{B}_{L,S,J,M_J} \equiv \{\mathcal{A}\tilde{\Psi}_{\gamma,L,S,J,M_J} | \gamma = (n_1, l_1, n_2, l_2) \text{ is compatible with } L, S\} , \tag{27}$$

where

$$\tilde{\Psi}_{\gamma,L,S,J,M_J} \equiv \sum_{M_S} \langle L, M_J - M_S, S, M_S | J, M_J \rangle \Psi_{\gamma,L,M_J-M_S,S,M_S} \ , \tag{28}$$

$$\Psi_{\gamma,L,M_L,S,M_S}(\boldsymbol{r}_1, \boldsymbol{r}_2) \equiv \Phi_{\gamma,L,M_L}(\boldsymbol{r}_1, \boldsymbol{r}_2) X_{S,M_S} \tag{29}$$

$$\begin{aligned} \Phi_{(n_1,l_1,n_2,l_2),L,M_L}(\boldsymbol{r}_1, \boldsymbol{r}_2) &\equiv \sum_{m_1,m_2} \langle l_1 m_1, l_2 m_2 | L M_L \rangle \phi_{n_1,l_1,m_1}(\boldsymbol{r}_1) \phi_{n_2,l_2,m_2}(\boldsymbol{r}_2) \\ &= \frac{u_{n_1 l_1}(r_1) u_{n_2 l_2}(r_2)}{r_1 r_2} Y_{l_1,l_2,L,M_L}(\hat{\boldsymbol{r}}_1, \hat{\boldsymbol{r}}_2) \ , \end{aligned} \tag{30}$$

and $Y_{l_1,l_2,L,M_L}(\hat{\boldsymbol{r}}_1, \hat{\boldsymbol{r}}_2), X_{S,M_S}$ are the coupled two-body orbit wavefunction and spin state (a rank-2 tensor with both 2-dimensional indices) respectively. By "compatible" I mean (1) $l_1 + l_2 \geq L \geq |l_1 - l_2|$ and (2) non-zero after antisymmetrization.

Note that $\langle j_2 m_2, j_1 m_1 | J M \rangle = (-1)^{J-j_1-j_2} \langle j_1 m_1, j_2 m_2 | J M \rangle$, the transposition causes

$$\mathcal{P}_{12} X_{S,M_S} = (-1)^{S-1} X_{S,M_S}, \tag{31}$$

$$\mathcal{P}_{12} Y_{l_1,l_2,L,M_L}(\hat{\boldsymbol{r}}_1, \hat{\boldsymbol{r}}_2) \equiv Y_{l_1,l_2,L,M_L}(\hat{\boldsymbol{r}}_2, \hat{\boldsymbol{r}}_1) = (-1)^{L-l_1-l_2} Y_{l_2,l_1,L,M_L}(\hat{\boldsymbol{r}}_1, \hat{\boldsymbol{r}}_2), \tag{32}$$

which gives

$$\mathcal{P}_{12} \Psi_{\gamma,L,S} = (-1)^{S+L-1-l_1-l_2} \Psi_{(n_2,l_2,n_1,l_1),L,S} \tag{33}$$

$$= \begin{cases} (-1)^{S+L-1} \Psi_{\gamma,L,S} & \text{if } n_1 = n_2, l_1 = l_2, \\ \text{Linear independent from } \Psi_{\gamma,L,S} & \text{otherwise,} \end{cases} \tag{34}$$

where $\Psi_{\gamma,L,S}$ stands for a generic state in the eigen subspace marked by γ, L, S whose special cases include $\tilde{\Psi}_{\gamma,L,S,J,M_J}$ and $\Psi_{\gamma,L,M_L,S,M_S}$. The normalization factor is thus

$$N_{\gamma,L,S} \equiv ||\Psi_{\gamma,L,S} - \mathcal{P}_{12} \Psi_{\gamma,L,S}||_2 = \begin{cases} 1 + (-1)^{S+L-1} & \text{if } n_1 = n_2, l_1 = l_2, \\ \sqrt{2} & \text{otherwise.} \end{cases} \tag{35}$$

A routine that is frequently adopted when calculating the matrix elements of a scalar symmetric observable $O, \mathcal{P}_{12} O = O$ comes as follow:

$$\begin{aligned} \langle \mathcal{A}\Psi' | O | \mathcal{A}\Psi \rangle &= \frac{2}{N'N} \left(\langle \Psi' | O | \Psi \rangle - \langle \Psi' | O | \mathcal{P}_{12} \Psi \rangle \right) \\ &= \frac{2}{N'N} \left(\langle \Psi' | O | \Psi \rangle + (-1)^{S+L-l_1-l_2} \mathcal{P}(n_1 \leftrightarrow n_2, l_1 \leftrightarrow l_2) \{ \langle \Psi' | O | \Psi \rangle \} \right), \end{aligned} \tag{36}$$

where $\mathcal{P}(n_1 \leftrightarrow n_2, l_1 \leftrightarrow l_2)$ swaps n_1, l_1 with n_2, l_2 in the sandwich, and Ψ', Ψ are shorthands for $\Psi_{\gamma',L',S'}, \Psi_{\gamma,L,S}$.

3.1 Matrix elements

Because ψ_{n,l,m,m_s} are degenerate over m, m_s, it is clear that

$$(h_0(1) + h_0(2)) \mathcal{A} \Psi_{(n_1,l_1,n_2,l_2),L,S} = (\epsilon_{n_1,l_1} + \epsilon_{n_2,l_2}) \mathcal{A} \Psi_{(n_1,l_1,n_2,l_2),L,S} \ . \tag{37}$$

3.1.1 Electronstatic interaction V

Separating variables

$$V(\boldsymbol{r}_1,\boldsymbol{r}_2)=\sum_{l=0}^{+\infty}\frac{4\pi\min(r_1,r_2)^l}{(2l+1)\max(r_1,r_2)^{l+1}}\sum_{m=-l}^{l}Y_{lm}(\hat{\boldsymbol{r}}_1)Y_{lm}(\hat{\boldsymbol{r}}_2)^*\ , \tag{38}$$

one obtains

$$\langle\Phi_{\gamma',L,M_L}|V|\Phi_{\gamma,L,M_L}\rangle=\sum_{l=0}^{+\infty}\mathrm{angulaV}(l,l_1',l_2',l_1,l_2;L,M_L)\mathrm{radiaV}(l,u_{n_1'l_1'},u_{n_2'l_2'},u_{n_1l_1},u_{n_2l_2}) \tag{39}$$

defining

$$\mathrm{angulaV}(l,l_1',l_2',l_1,l_2;L,M_L)\equiv\sum_{m=-l}^{l}\int\mathrm{d}\Omega_1\int\mathrm{d}\Omega_2 Y_{l_1',l_2',L,M_L}(\hat{\boldsymbol{r}}_1,\hat{\boldsymbol{r}}_2)^*Y_{l,m}(\hat{\boldsymbol{r}}_2)^*Y_{l,m}(\hat{\boldsymbol{r}}_1)Y_{l_1,l_2,L,M_L}(\hat{\boldsymbol{r}}_1,\hat{\boldsymbol{r}}_2), \tag{40}$$

$$\mathrm{radiaV}(l,u_{1'},u_{2'},u_1,u_2)\equiv\int_0^{+\infty}\mathrm{d}r_1\int_0^{+\infty}\mathrm{d}r_2u_{1'}(r_1)u_{2'}(r_2)\frac{4\pi\min(r_1,r_2)^l}{(2l+1)\max(r_1,r_2)^{l+1}}u_1(r_1)u_2(r_2)\ . \tag{41}$$

Further evaluation of angular$(l,l_1',l_2',l_1,l_2;L,M_L)$ into Wigner-3j symbols (See App. B.1) shows that $l\in[|l_1'-l_1|,l_1'+l_1]\cap[|l_2'-l_2|,l_2'+l_2]$ is necessary for its being non-zero, so the summation over l in Eq. (40) is finite.

Moreover, V is isotropic and has nothing to do with the spin. Therefore the degeneracy over M_L,M_S is preserved in the representation of V. Namely, the V matrix is independent of M_L,M_S. Thus I can compute it in the $M_L=L$ subspace for simplicity and denote

$$\langle\gamma',L|V|\gamma,L\rangle\equiv\sum_{l=0}^{+\infty}\mathrm{angulaV}(l,l_1',l_2',l_1,l_2;L,L)\mathrm{radiaV}(l,u_{n_1'l_1'},u_{n_2'l_2'},u_{n_1l_1},u_{n_2l_2})\ , \tag{42}$$

and I have $\langle\tilde{\Psi}_{\gamma',L,S,J,M_J}|V|\tilde{\Psi}_{\gamma,L,S,J,M_J}\rangle=\langle\gamma',L|V|\gamma,L\rangle$ because $\{\tilde{\Psi}_{\gamma',L,S,J,M_J}|J,M_J\}$ is unitarily transformed from $\{\Psi_{\gamma,L,M_L,S,M_S}|M_L,M_S\}$.

Since V is symmetric, one adopts Eq. (36),

$$\begin{aligned}&\langle\mathcal{A}\tilde{\Psi}_{\gamma',L,S,J,M_J}|V|\mathcal{A}\tilde{\Psi}_{\gamma,L,S,J,M_J}\rangle\\=&\frac{2}{N_{\gamma',L,S}N_{\gamma,L,S}}(\langle\gamma',L|V|(n_1,l_1,n_2,l_2),L\rangle+(-1)^{S+L-l_1-l_2}\langle\gamma',L|V|(n_2,l_2,n_1,l_1),L\rangle)\end{aligned} \tag{43}$$

3.1.2 Spin-orbit coupling

It is generally observed that $0=[\boldsymbol{s}_{k_1}\cdot\boldsymbol{l}_{k_2},\boldsymbol{l}_{k_3}^2]\ \forall k_1,k_2,k_3\in\{1,2\}$, which results in that H_{SOC} commutes with $\boldsymbol{l}_1^2,\boldsymbol{l}_2^2$ aside from $\boldsymbol{L}^2,\boldsymbol{S}^2,\boldsymbol{J}$. Adopting the routine in Eq. (36) and dropping out the

inter-electron spin-orbit coupling, one turns to

$$\begin{aligned}&\langle\tilde{\Psi}_{\gamma',L,S,J,M_J}|\sum_{k=1,2}\xi(r_k)\boldsymbol{s}_k\cdot\boldsymbol{l}_k|\tilde{\Psi}_{\gamma,L,S,J,M_J}\rangle\\=&\sum_{k=1}^{2}\text{angulaSO}(l_1,l_2;L,S,J,M_J;k)\delta_{l_1',l_1}\delta_{l_2',l_2}\text{radiaSO}(u_{n_1'l_1'},u_{n_2'l_2'},u_{n_1l_1},u_{n_2l_2};k)\ ,\end{aligned}\tag{44}$$

where

$$\begin{aligned}&\text{angulaSO}(l_1,l_2;L,S,J,M_J;k)\\&\quad=\sum_{M_L',M_S',M_L,M_S}\langle L,M_L',S,M_S'|J,M_J\rangle\langle L,M_L,S,M_S|J,M_J\rangle\\&\quad\int\mathrm{d}\Omega_1\int\mathrm{d}\Omega_2 Y_{l_1,l_2,L,M_L'}(\hat{\boldsymbol{r}}_1,\hat{\boldsymbol{r}}_2)^*X^\dagger_{S,M_S'}\boldsymbol{s}_k\cdot\boldsymbol{l}_kY_{l_1,l_2,L,M_L}(\hat{\boldsymbol{r}}_1,\hat{\boldsymbol{r}}_2)X_{S,M_S}\ ,\end{aligned}\tag{45}$$

$$\text{radiaSO}(u_{1'},u_{2'},u_1,u_2;k)=\int_0^{+\infty}\mathrm{d}r_1\int_0^{+\infty}\mathrm{d}r_2u_{1'}(r_1)u_{2'}(r_2)\xi(r_k)u_1(r_1)u_2(r_2)\ .\tag{46}$$

The details about implementing these functions can be found in App. B.2 , where it is also observed that $S=0$ suffices angula$(l_1,l_2;L,S,J,M_J;k)=0$. Therefore for singlet computation of V matrix is enough for the diagonalization.

3.2 Organizing basis

To diagonalize the Hamiltonian, $\mathcal{B}$ should be truncated, leaving those electron configurations that are relevant to the state of interest. To avoid double counting when enumerating the electron configurations, in practice it is arranged so that $n_1+0.7l_1<n_2+0.7l_2$ or $n_1+0.7l_1=n_2+0.7l_2$ and $n_1<n_2$. Different electron configurations in the basis are not intentionally ordered.

3.2.1 Evaluating the singlet states

To verify the precision of the method, the experimental values and computational results of some states are listed in Tab. The experimental value of the ground state $\gamma=(4,0,4,0),L=0,S=0$ energy is -0.6609. Under the basis whose $n_1,n_2\in\{3,4,5\}$, the computed ground energy is -0.6607. This result can be directly obtained as one runs `./LS.py`.

Table 3: Experimental values and computational results of four interested states

State	Experimental (in a.u.)	Computational (in a.u.)	Basis
4s4s $^1S_0$	-0.6609	-0.6607	$n_1,n_2\in\{3,4,5\}$
4s4p $^1P_1$	-0.5532	-0.5491	
4s18s $^1S_0$	-0.4383	-0.4430	$n_1=4,l_1=0,n_2\in\{4,5,\cdots,55\},l_2=0$
4s16d $^1D_2$	-0.4385		

Other states can be solved in similar ways, e.g. the solved energy of $\gamma=(4,0,18,0),L=0,S=0$ is -0.4430, which is close to the experimental value -0.4383 .

The precision of the solved energies for $L=0,S=0$ states verifies that both the method and the numerical implementations are reliable. Thus the corresponding state vectors are reliable in the

following computation. Spin-orbit coupling has not been included so far. That is also why I chose $^1S_0$ states for verification, for spin-orbit coupling has the least effect on them.

4 Quantities of Interest

4.1 Energy difference between states of interest

4.2 Stark shift of high Rydberg states

4.3 Linewidth of high Rydberg states

References

[1] "Atomic units - wikipedia."

[2] J. Sugar and C. Corliss, "Energy levels of calcium, ca i through ca xx," *Journal of Physical and Chemical Reference Data*, vol. 8, no. 3, pp. 865–916, 1979.

[3] M. Aymar and M. Telmini, "Eigenchannel r-matrix study of the j=0 and j=2 even parity spectra of calcium below the ca+ 3d3/2 threshold," *Journal of Physics B: Atomic, Molecular and Optical Physics*, vol. 24, pp. 4935–4956, dec 1991.

[4] Y. Singh, B. K. Sahoo, and B. P. Das, "Correlation trends in the ground-state static electric dipole polarizabilities of closed-shell atoms and ions," *Phys. Rev. A*, vol. 88, p. 062504, Dec 2013.

[5] U. Öpik, "The polarization of a closed-shell core of an atomic system by an outer electron II. evaluation of the polarizabilities from observed spectra," *Proceedings of the Physical Society*, vol. 92, pp. 566–572, nov 1967.

A Subroutine for $A \cdot x = \lambda M \cdot x$

B Implementation of angular and radial integration

B.1 angulaV

$$Y_{l_1,l_2,L,M_L}(\hat{\boldsymbol{r}}_1,\hat{\boldsymbol{r}}_2) = \sum_{m_1} \langle l_1, m_1, l_2, (M_L - m_1)|L, M_L\rangle Y_{l_1,m_1}(\hat{\boldsymbol{r}}_1) Y_{l_2,M_L-m_1}(\hat{\boldsymbol{r}}_2) \ . \tag{47}$$

$$\begin{aligned}\text{angulaV}(l,l_1',l_2',l_1,l_2;L,M_L) = &\sum_{m=-l}^{l}\sum_{m_1'}\langle l_1',m_1',l_2',(M_L-m_1')|L,M_L\rangle\sum_{m_1}\langle l_1,m_1,l_2,(M_L-m_1)|L,M_L\rangle\\ &\int \mathrm{d}\Omega_1 Y^*_{l_1',m_1'}Y_{l,m}Y_{l_1,m_1}\int \mathrm{d}\Omega_2 Y^*_{l_2',M_L-m_1'}Y^*_{l,m}Y_{l_2,M_L-m_1} \qquad (48)\\ =&\sum_{m_1'}\langle l_1',m_1',l_2',(M_L-m_1')|L,M_L\rangle\sum_{m_1}\langle l_1,m_1,l_2,(M_L-m_1)|L,M_L\rangle(-1)^{M_L+m_1'-m_1}\\ &G(l_1',l,l_1;-m_1',m_1'-m_1,m_1)G(l_2',l,l_2;-M_L+m_1',m_1-m_1',M_L-m_1)\\ &\mathbb{I}(l\geq|m_1'-m_1|)\ , \qquad (49)\end{aligned}$$

$$\begin{aligned}G(l_1,l_2,l_3;m_1,m_2,m_3) &\equiv \int \mathrm{d}\Omega_1 Y_{l_1,m_1}Y_{l_2,m_2}Y_{l_3,m_3} \qquad (50)\\ &= \sqrt{\frac{(2l_1+1)(2l_2+1)(2l_3+1)}{4\pi}}\begin{pmatrix} l_1 & l_2 & l_3\\ 0 & 0 & 0\end{pmatrix}\begin{pmatrix} l_1 & l_2 & l_3\\ m_1 & m_2 & m_3\end{pmatrix}\ , \qquad (51)\end{aligned}$$

where the Wigner-3j symbol, if nonzero, requires $m_1+m_2+m_3=0$ and that l_1,l_2,l_3 comprise a triangle. Thus in Eq. (49), l is bounded by l_1,l_2,l_1',l_2' as well.

For numerical efficiency, the $l_1=l_2$ case is specially treated because the result of angular integration could be reused. Please refer to the code `./Dev/LS.py`.

B.2 angulaSO

$$\begin{aligned}Y_{l_1,l_2,L,M_L}(\hat{\boldsymbol{r}}_1,\hat{\boldsymbol{r}}_2)X_{S,M_S} = &\sum_{m_1,m_2}\sum_{m_{s1},m_{s2}}\langle l_1,m_1,l_2,m_2|L,M_L\rangle Y_{l_1,m_1}(\hat{\boldsymbol{r}}_1)Y_{l_2,m_2}(\hat{\boldsymbol{r}}_2)\\ &\langle\frac{1}{2},m_{s1},\frac{1}{2},m_{s2}|S,M_S\rangle\chi(m_{s1})\otimes\chi(m_{s2}) \qquad (52)\end{aligned}$$

$$\begin{aligned}&\text{angulaSO}(l_1,l_2;L,S,J,M_J;k)\\ &\quad=\sum_{M_L',M_S',M_L,M_S}\langle L,M_L',S,M_S'|J,M_J\rangle\langle L,M_L,S,M_S|J,M_J\rangle\\ &\quad\int \mathrm{d}\Omega_1\int \mathrm{d}\Omega_2 Y_{l_1,l_2,L,M_L'}(\hat{\boldsymbol{r}}_1,\hat{\boldsymbol{r}}_2)^* X^\dagger_{S,M_S'}\boldsymbol{s}_k\cdot\boldsymbol{l}_k Y_{l_1,l_2,L,M_L}(\hat{\boldsymbol{r}}_1,\hat{\boldsymbol{r}}_2)X_{S,M_S} \qquad (53)\\ &=\sum_{M_L',M_S',M_L,M_S}\langle L,M_L',S,M_S'|J,M_J\rangle\langle L,M_L,S,M_S|J,M_J\rangle\\ &\quad\sum_{m_{l2}}\langle l_1,(M_L'-m_{l2}),l_2,m_{l2}|LM_L'\rangle\langle l_1,(M_L-m_{l2}),l_2,m_{l2}|LM_L\rangle\\ &\quad\sum_{m_{s2}}\langle\frac{1}{2},(M_S'-m_{s2}),\frac{1}{2},m_{s2}|SM_S'\rangle\langle\frac{1}{2},(M_S-m_{s2}),\frac{1}{2},m_{s2}|SM_S\rangle\\ &\quad\int \mathrm{d}\Omega_1 Y_{l_1,M_L'-m_{l2}}(\hat{\boldsymbol{r}}_1)^*\chi(M_S'-m_{s2})^\dagger\boldsymbol{s}_1\cdot\boldsymbol{l}_1 Y_{l_1,M_L-m_{l2}}(\hat{\boldsymbol{r}}_1)\chi(M_S-m_{s2})\ , \qquad (54)\end{aligned}$$

$$\int \mathrm{d}\Omega Y_{l,m_l'}(\hat{\boldsymbol{r}})^* \chi(m_s')^\dagger \boldsymbol{s}\cdot\boldsymbol{l} Y_{l,m_l}(\hat{\boldsymbol{r}})\chi(m_s) = \delta_{m_l,m_l'}\delta_{m_s,m_s'} m_l m_s$$
$$+\frac{1}{2}\sum_{\mu=\pm 1}\delta_{m_l+\mu,m_l'}\delta_{m_s-\mu,m_s'}\sqrt{(l(l+1)-m_l(m_l+\mu))\left(\frac{3}{4}-m_s(m_s-\mu)\right)} \tag{55}$$

This angular integration is zero when $S=0$. As $M_S'=M_S=0$ in the summation of Eq. (53) , thus $M_L'=M_J=M_L$ and the summation over $m_{s2}=\pm\frac{1}{2}$ is 0 because the integration over $\hat{\boldsymbol{r}}_1$ is $-(M_J-m_{l2})m_{s2}$. When $L=0$